



The adduct formation between the thioguanine-polyamine ligands and DNA with the AP site under UVA irradiated and non-irradiated conditions

Yukiko S. Abe, Shigeki Sasaki*

Graduate School of Pharmaceutical Sciences, Kyushu University, 3-1-1 Maidashi, Higashi-ku, Fukuoka 812-8582, Japan

ARTICLE INFO

Keywords:

AP site repair inhibition
Binding ligand
 α,β -unsaturated aldehyde
Covalent bond formation
Thioguanine

ABSTRACT

The AP sites are representative of DNA damage and known as an intermediate in the base excision repair (BER) pathway which is involved in the repair of damaged nucleobases by reactive oxygen species, UVA irradiation, and DNA alkylating agents. Therefore, it is expected that the inhibition or modulation of the AP site repair pathway may be a new type of anticancer drug. In this study, we investigated the effects of the thioguanine-polyamine ligands (^SG-ligands) on the affinity and the reactivity for the AP site under UVA irradiated and non-irradiated conditions. The ^SG-ligands have a photo-reactivity with the A-F-C sequence where F represents a tetrahydrofuran AP site analogue. Interestingly, the ^SG-ligands promoted the β -elimination of the AP site followed by the formation of a covalent bond with the β -eliminated fragment without UVA irradiation.

1. Introduction

DNA is continuously damaged by either endogenous or exogenous factors such as reactive oxygen species, UVA irradiation, DNA alkylating agents, etc.^{1,2} Damaged nucleobases are removed in the base excision repair (BER) pathway to form apurinic/aprimidinic sites (AP sites) as the intermediates.^{3,4} The AP site per se represents DNA damage and generated by spontaneous hydrolysis of the nucleobase at the rate of about 10^5 sites per day in human cells. As the accumulation of the AP sites enhances the cytotoxicity and mutagenicity, the AP site is immediately repaired by the highly-coordinated BER pathway.⁵ In other words, the blocking of the BER pathway is expected to enhance the cytotoxic efficacy of the AP sites.

Over the last 20 years, many approaches have attempted to develop the AP sites-binding molecules as therapeutic agents for cancer.^{6,7} Lhomme and co-workers developed intercalator-polyamine-nucleobase conjugates, which efficiently recognized and cleaved the AP sites.⁸ Recently, Brabec and co-workers also demonstrated that the metallohelices bind to the AP sites with a high affinity and inhibit the activity of human AP endonuclease 1 (APE1).⁹ APE1 is one of the most important enzymes in the BER pathway, which recognizes the AP sites and generates a single strand break with a 5'-deoxyribose phosphate end and a 3'-hydroxyl end as a result of the cleavage on the 5' side of the AP site. The generated 3'-hydroxyl end is processed either by adding several nucleotides or by a single nucleotide replacement. The APE1 inhibitors increase the cytotoxicity by the accumulation of AP sites and

have the potential to become a new class of anticancer drugs. Granzhan and co-workers suggested that the bis-naphthalene macrocycles bind to the AP site analogues with a high affinity and inhibit their cleavage by APE1.¹⁰ They also indicated that the bis-naphthalene ligand promoted β -elimination of the AP site, and subsequently, formed the adduct with the produced α,β -unsaturated aldehyde.¹¹ A similar approach for inhibition of the AP site repair was reported by McCullough and Lloyd and they developed small molecules that catalyze the DNA strand cleavage at the AP sites.¹² Their compound promotes the β - and δ -elimination reaction at the AP sites via the formation of a Schiff base. Both the β -eliminated products at the AP sites and the adducts with the ligand act as the 3'-block for the subsequent polymerization in the AP site repair system.

We have previously reported that the nucleobase-polyamine conjugates bind to the AP sites and cleaved DNA at the AP site by promoting β -elimination.^{13,14} The ligands conjugating the adenine, guanine, cytosine or thymine base showed a selectivity to the opposing base of the AP sites according to the Watson-Crick base pairing. These ligands showed no binding for the full match ODNs without AP sites.¹³ The ligand binding affinity was supported by nonspecific electrostatic interactions between the polyamine part and DNA phosphate backbone. The polyamine part was also essential for promoting β -elimination. Thus, the A-n3-ligand conjugating the adenine with 3,3'-diaminodipropyl-amine effectively and selectively promoted the DNA cleavage at the AP site with the opposing dT. On the other hand, the G-n3-ligand did not show a selectivity in the cleavage of the DNA at the AP sites. In

* Corresponding author.

E-mail address: sasaki@phar.kyushu-u.ac.jp (S. Sasaki).

<https://doi.org/10.1016/j.bmc.2019.115160>

Received 25 July 2019; Received in revised form 7 October 2019; Accepted 9 October 2019

Available online 31 October 2019

0968-0896/ © 2019 Elsevier Ltd. All rights reserved.

this study, we attempted to improve the property of the G-n3-ligand regarding selectivity and reactivity toward the AP site. As the thioguanine base is known to form a photo-crosslink with the DNA base by UVA irradiation,^{15,16} we expected that the thioguanine base would form a covalent bond with DNA having the AP site by UVA irradiation. The 6-S of the thioguanine base has a higher nucleophilicity than 6-O of the guanine, leading to the expectation to form an adduct with the unsaturated aldehyde produced *via* the β -elimination of the AP site.

2. Results and discussion

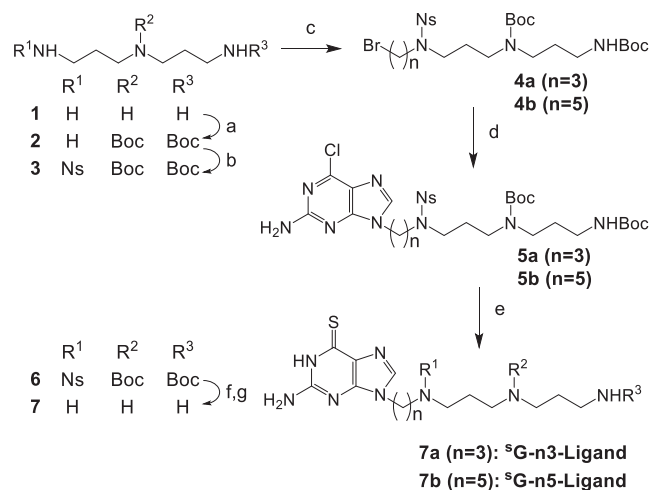
2.1. Design and synthesis of the thioguanine-polyamine conjugates

It is known that the thiocarbonyl group of the thioguanine base reacts with the 5,6-double bond of the thymine and cytosine base by UVA irradiation.¹⁶ Therefore, it was expected that, when the thioguanine base enters the space of the AP site, the photo-crosslinking reaction would occur by UVA irradiation between the thiocarbonyl part and the DNA base in a closer proximity of the ligand in the AP sites.

Two ligands with different lengths of the linker between the thioguanine base and the 3,3'-diaminodipropylamine were synthesized (Scheme 1). 3,3'-Diaminodipropylamine (**1**) was protected with the *t*-butoxycarbonyl (Boc) and the Nosyl (Ns) groups in 2 steps to give **3**.¹³ 1,3-Dibromopropane or 1,5-dibromopentane was reacted with **3** to form the triamine bromide (**4**), which was conjugated with 2-amino-6-chloropurine to produce **5**. The 6-chloro group of **5** was replaced by thiourea in ethanol to yield **6**, which was subjected to the deprotection of the Ns and Boc groups to produce the desired ^sG-ligand (**7**). Each ligand was purified as hydrochloride salts. The ligand **7** was labelled according to the length of the spacer: ^sG-n3-ligand and ^sG-n5-ligand conjugated with the propyl (n = 3) and the pentyl linker (n = 5), respectively.

2.2. Effects of ^sG-n3- and ^sG-n5-ligands on the thermal stability of the duplex ODNs containing the AP site

It was expected that thioguanine would form a base-pair with dC opposite of the AP site,¹⁷ and the binding property of the ^sG-ligands was evaluated by measuring the melting temperature (T_m) in the absence and presence of the ^sG-ligands (Table 1). The duplexes (**1**–**6**) are



Scheme 1. The synthesis of ^sG-ligands. (a) i) CF₃CO₂Et, MeOH, -78 °C to 0 °C ii) (Boc)₂, 0 °C to rt iii) LiOH/H₂O, THF, rt, 57%; (b) NsCl, Et₃N, CH₂Cl₂, 0 °C, 75%; (c) n = 3; 1,3-dibromopropane, K₂CO₃, MeCN, rt, 67%, n = 5; 1,5-dibromopentane, K₂CO₃, DMF, rt, 93%; (d) 2-amino-6-chloropurine, K₂CO₃, DMF, 0 °C to rt, n = 3; 82%, n = 5; 74%; (e) thiourea, EtOH, reflux, n = 3; 73%, n = 5; 80%; (f) thiophenol, K₂CO₃, DMF, rt, n = 3; 94%, n = 5; 91%; (g) 0.5 M HCl/MeOH, rt, n = 3; quant., n = 5; 78%.

composed of the AP site with the tetrahydrofuran derivative (F) and dA, dG, dT dC at its opposing site Z, which is located in the flanking 5'-, and 3'-sequences (5' GCGTAX₁-F-Y₁ATGCG 3'/3' CGCATX₂-Z-Y₂TACGC 5') (Tables 1 and 2). The ^sG-n3- and ^sG-n5-ligands did not significantly increase the T_m values of any of the fully matched sequences (Table 3). In the same flanking (A-F-C/T-Z-G) sequences (duplexes **1**–**4**), the ^sG-n3-ligand showed the highest ΔT_m value to the cytosine base at Z (duplex **4**). Although the selectivity of the ^sG-n3-ligand for Z = dC is the same as that obtained with the corresponding G-ligand, its dC-selectivity and stabilizing effect were slightly lower than those of the G-n3-ligand (ΔT_m : ^sG-n3-ligand: +5.4 °C, G-n3-ligand: +6.6 °C).¹³ This may be due to the lower thermal stability of the ^sG/C pair than that of the G/C pair.¹⁸ The flanking sequences of the AP site with the F/C combination (duplexes **4**–**6**) affected the stabilizing effect of the ^sG-n3-ligand in the order of duplex **4** (A-F-C/T-Z-G) > duplex **5** (C-F-A/G-Z-T) > duplex **6** (A-F-A/T-Z-T). This stability trend agrees with the assumption based on the nearest neighbor parameters for the Watson-Crick duplex, in which the base pair between dC and thioguanine at the AP site is treated as a G/C base pair.¹⁹ In contrast, the ^sG-n5-ligand indicated a broader selectivity. Although the stability trend is similar to that with the ^sG-n3-ligand, there was no significant difference between the sequences. Due to the flexible pentyl linker of the ^sG-n5-ligand, a variety of base pairs including the ^sG/C Watson-Crick type base pair, the ^sG/G Hoogsteen base pair, the ^sG/T wobble base pair etc., might contribute to its stability of the different sequences.

2.3. The effect of UVA irradiation on duplexes containing AP site analogue with ^sG-n3- and ^sG-n5-ligands

The photo-crosslinking reaction was performed by the UVA irradiation (4 W, 365 nm) of a solution of the ^sG-ligand (100 μ M) and the duplex (10 μ M) in a buffer containing 10 mM HEPES-NaOH (pH 7.0), 5 mM DTT and 100 mM NaCl, and followed by an HPLC analysis (Fig. 1). DTT was added to enhance the photoreaction.²⁰ The strand of the duplex is labelled according to the flanking bases, such as “the AFC strand” for 5'-d(GCGTAA FCATGCG)-3'. In the HPLC, the peaks of the two strands of duplexes **1** and **3** are overlapped, and those of duplexes **2**, **4**, **5** and **6** appeared as two peaks. The HPLC charts of duplexes **1**–**3** did not change after a 24-hour irradiation (Fig. 1(A)–(C)). In remarkable contrast, duplex **4** (Z = dC) produced a new peak marked with (*) after 24 h and accompanied by a decrease in the AFC strand (Fig. 1D), indicating the reaction selectivity to the AP site with the opposing dC. The photoreaction slowly proceeded and the new peak appeared after 3 h, then gradually increased (Fig. S2). Duplexes **5** or **6** having different flanking base pairs at the F/C showed no indication of a photoreaction by the ^sG-n3-ligand (Fig. 1(E) and (F)). The photoreaction for duplex **4** (Z = dC) selectively took place with the ^sG-n5-ligand albeit with a lower efficiency than that of the ^sG-n3-ligand (Fig. 1(G)). These results indicated that the photo-reactivity depends not only on the binding to the AP site but also the flanking bases. In the control experiment, the G-n3-ligand conjugating the natural guanine base did not produce photo-products (Fig. 1(H)), indicating that the thiocarbonyl part played an important role in the photoreaction.

The molecular mass of the new peak marked with (*) in Fig. 1D was measured by MALDI-TOF/MS to be 4157.23, which indicated that the structure suffered desulfurization of the adduct between the AFC strand and the ^sG-n3-ligand (Fig. S3). Although isolation and determination of the adduct structure was unsuccessful, its structure was considered as follows. It was speculated based on the photo-reactivity of the thiocarbonyl group that a thietane intermediate formed between the 5,6-double bond of dC in the AFC strand and the thiocarbonyl group of the thioguanine base, and that the thietane intermediate further proceeded to the ring opening and the subsequent dehydrosulfurization reaction (Chart S1).¹⁵ Such a thietane formation is possible when the thiocarbonyl of thioguanine approaches the 5,6-double bond of dC on the 3' side of the AP site from the major groove (Figs. S1, A and B). This

Table 1Increase of the UV melting temperature (ΔT_m (\pm SD), $^{\circ}$ C).

	Duplex (X_1 -F- Y_1 / X_2 -Z- Y_2) (T_m $^{\circ}$ C in the absence of the ligand)					
	1	2	3	4	5	6
	A-F-C/T-A-G (33.6 (\pm 0.2))	A-F-C/ T-G-G (34.4 (\pm 0.2))	A-F-C/T-T-G (33.0 (\pm 0.4))	A-F-C/T-C-G (30.7 (\pm 0.3))	C-F-A/ G-C-T (32.0 (\pm 0.4))	A-F-A/T-C-T (29.9 (\pm 0.3))
$^{\text{S}}\text{G-n3-ligand}$	+2.3 (\pm 0.5)	+1.6 (\pm 0.1)	+1.2 (\pm 0.9)	+5.4 (\pm 0.3)	+3.5 (\pm 0.6)	+1.8 (\pm 0.7)
$^{\text{S}}\text{G-n5-ligand}$	+2.8 (\pm 0.2)	+3.8 (\pm 1.6)	+3.1 (\pm 1.0)	+4.2 (\pm 1.1)	+4.1 (\pm 0.7)	+3.3 (\pm 1.3)

The UV-melting curves were measured in 10 mM HEPES-NaOH buffer (pH 7.0) containing 100 mM NaCl at the scan rate of 1 $^{\circ}$ C at 260 nm in the absence and presence of the $^{\text{S}}\text{G}$ -ligands. [duplex ODNs]: 2 μM , [$^{\text{S}}\text{G}$ -ligands]: 10 μM . F denotes tetrahydrofuran as the stable AP site analogue. The melting temperature of the duplexes in the absence of ligand is shown in the parenthesis. The average mean and the standard deviation, ΔT_m (\pm SD), were calculated based on three independent experiments.

Table 2

MALDI-TOF/MS of the synthesized ODNs.

Sequence	5'-d(GCG TAX ₁ F Y ₁ AT GCG)-3'	Calcd. [M-H] ⁻	Found
A-F-C	5'-d(GCG TAA F CAT GCG)-3'	3847.7	3847.6
C-F-A	5'-d(GCG TAC F AAT GCG)-3'	3847.7	3847.7
A-F-A	5'-d(GCG TAA F AAT GCG)-3'	3871.7	3871.7

Table 3Melting temperature of full match duplexes and ΔT_m values obtained using $^{\text{S}}\text{G}$ -ligands.

X_1 -N- Y_1 / X_2 -N- Y_2	T_m ($^{\circ}$ C)	+ $^{\text{S}}\text{G-n3-ligand}$		+ $^{\text{S}}\text{G-n5-ligand}$	
		ΔT_m (\pm SD) ($^{\circ}$ C)	ΔT_m (\pm SD) ($^{\circ}$ C)	ΔT_m (\pm SD) ($^{\circ}$ C)	ΔT_m (\pm SD) ($^{\circ}$ C)
A-T-C/T-A-G	52.0 (\pm 0.1)	+0.5 (\pm 0.2)	+0.6 (\pm 0.1)		
A-C-C/T-G-G	54.8 (\pm 0.0)	+0.5 (\pm 0.2)	+1.0 (\pm 0.2)		
A-A-C/T-T-G	52.1 (\pm 0.1)	+0.2 (\pm 0.3)	+0.7 (\pm 0.3)		
A-G-C/T-C-G	48.5 (\pm 0.1)	+0.7 (\pm 0.2)	+0.6 (\pm 0.1)		
C-G-A/G-C-T	55.2 (\pm 0.1)	+0.4 (\pm 0.2)	+0.9 (\pm 0.2)		
A-G-A/T-C-T	50.3 (\pm 0.1)	+0.7 (\pm 0.2)	+0.6 (\pm 0.1)		

Duplexes are 5'-d(GCG TA X₁ N Y₁AT GCG)-3' and 3'-d(GCG ATX₂ N Y₂TA GCG)-5'. Each melting curve was measured in the absence and presence of 10 μM ligand, at a concentration of 2 μM duplex in the buffer containing 10 mM HEPES-NaOH (pH 7.0), 100 mM NaCl, respectively.

speculation may account for the fact that the $^{\text{S}}\text{G-n3-ligand}$ did not form a photo-adduct for the CFA strand, in which the thiocarbonyl of thio-guanine is in an opposite direction to the 5,6-double bond of dC on the 5' side of the AP site (Figs. S1, C and D).

2.4. The DNA cleavage and adduct forming reaction of the AP sites with the $^{\text{S}}\text{G-n3-}$ and $^{\text{S}}\text{G-n5-ligands}$

The $^{\text{S}}\text{G}$ -ligands were next subjected to investigation for the DNA cleavage and adduct forming reaction of the AP site. The single-stranded 5' FAM-DNA1(U) containing the uracil residue was used to produce the AP site. The DNA1(U) was annealed with DNA2(X), which was treated with uracil-DNA glycosylase to create the DNA1(AP)/DNA2(X) duplex having an AP site. The cleaved fragments of 5' FAM-DNA1(AP) were analyzed by gel-electrophoresis, which were visualized by FAM fluorescence. The reactions were performed using the $^{\text{S}}\text{G-n3-}$ and $^{\text{S}}\text{G-n5-ligands}$ and all four AP/X combinations (X = dA, dG, dT, dC) and all the gel images are shown in Fig. S4. Fig. 2 illustrates the typical results using gels obtained with the AP/C combination and the control experiment using the G-n3-ligand conjugating a guanine base. Fig. 2 also summarizes the time course of the reaction of all combinations. The plausible reaction scheme of the $^{\text{S}}\text{G}$ -ligands with DNA via β - and δ -elimination of the AP site is summarized in Chart 1.^{21–23}

The AP site of DNA1 is in equilibrium with the open-chain aldehyde DNA3, which undergoes β -elimination of its 3'-O-phosphate by the attack of the amine base of the ligand to produce DNA4 and DNA5. DNA4a is in equilibrium with DNA6, which produced DNA7 via δ -elimination.¹⁴ DNA4a is also in equilibrium with the hydrated form

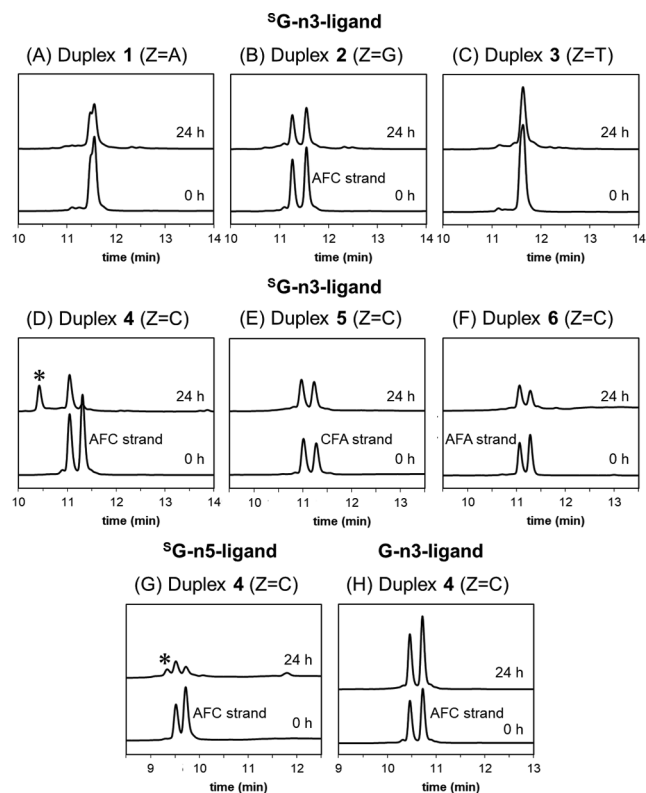


Fig. 1. HPLC analysis of the reaction between the $^{\text{S}}\text{G-n3-ligand}$ and (A) duplex 1, (B) duplex 2, (C) duplex 3, (D) duplex 4, (E) duplex 5, (F) duplex 6. (G) The reaction between the $^{\text{S}}\text{G-n5-ligand}$ and duplex 4. (H) The reaction between G-n3-ligand and duplex 4. (5'-d(GCG TAX₁ F Y₁AT GCG)-3' / 3'-d(GCG ATX₂ Z Y₂TA GCG)-5', F = tetrahydrofuran.

DNA4b.²⁴ As a low selectivity in the DNA cleavage was observed for the opposing base at the AP site with the G-n3-ligand in a previous study,¹⁴ the effects of the flanking bases were not investigated in this study. Fig. 2A illustrates the time course of the reaction using the $^{\text{S}}\text{G-n3-ligand}$ and DNA with the AP/C combination. The fast-moving bands observed at 30 min correspond to the β -eliminated product DNA4 and the faster-moving bands became larger after a longer reaction time that indicated the δ -eliminated product DNA7. After 1 h, the slower-moving bands increased. Considering that the slower moving bands were not observed in the presence of the G-n3-ligand (Fig. 2B), and that these bands increased as the β -elimination bands of DNA4 decreased, this slower band was postulated to be due to the adduct of the $^{\text{S}}\text{G-n3-ligand}$ as shown in DNA8. The time course of the ratio of the DNA fragments observed in Fig. 2A is summarized in Fig. 2D, showing that DNA4 was initially formed, followed by the formation of DNA8 at a faster rate and DNA7 at a slower rate. Fig. 2E shows the time course of the reaction of the $^{\text{S}}\text{G-n3-ligand}$ with the AP/A combination. In this case, the DNA8 formation was much slower and DNA4 remained. In contrast, for the

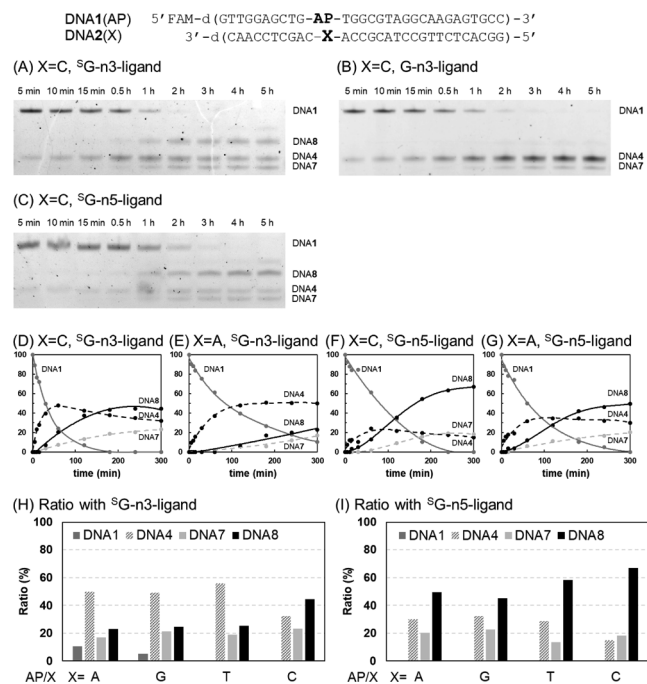


Fig. 2. The reaction analysis of the DNA cleavage in the presence of the ^SG -ligand or G-n3-ligand at interval times (A)–(C). The bands of the gel-images were quantified and their ratios (%) are plotted versus time (D)–(G). The fragment ratios observed after 6 h for all AP-X combination are summarized in (H) and (I). The reaction was performed using 100 nM duplexes at 37 °C in the presence of 10 μM ^SG -ligand and the products were resolved by 12% denaturing polyacrylamide gel electrophoresis containing 8 M urea at 25 mA for 40 min. The gel was visualized by FAM fluorescence using LAS-4000.

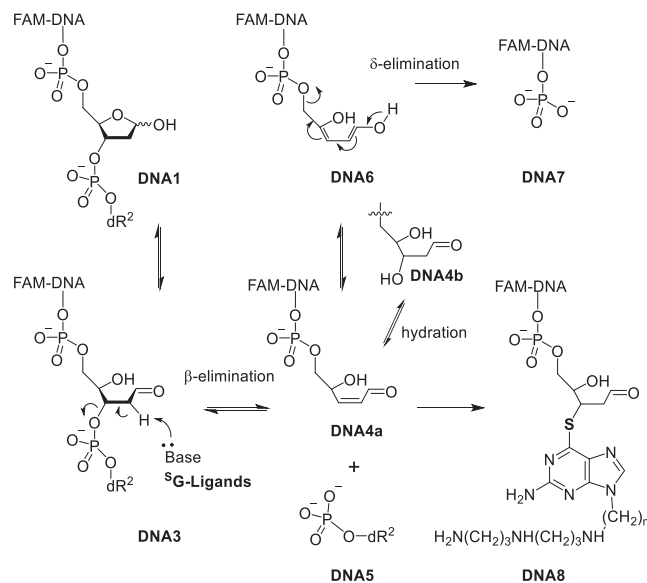


Chart 1. The postulated products via β -, δ -elimination in the presence of the ^SG -ligands. The β -eliminated product **4a** is in equilibrium with the hydrated **4b**.²⁴ The aldehyde may be in equilibrium also with the 5-membered form and the hydrated form.

reaction of the ^SG -n5-ligand with the AP/C combination, DNA8 formed at a faster reaction rate (Fig. 2C), in which the adduct formation proceeded without accumulation of the β -eliminated product DNA4 as shown in Fig. 2F. In the reaction of the ^SG -n5-ligand with the AP/A combination, the DNA8 formation was slower, and DNA4 remained to some extent (Fig. 2G).

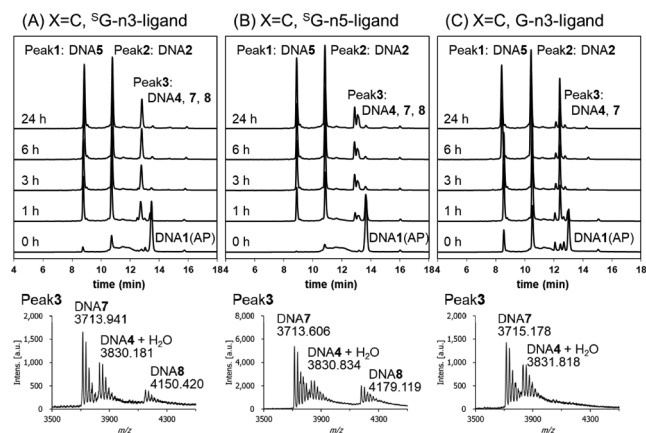


Fig. 3. The HPLC analysis of the reaction between the ^SG -ligands or G-n3-ligand and FAM-DNA1(AP)/DNA2(C) duplex (top) and the MS spectra of each peak 3 (bottom). HPLC condition: column; Waters \times Bridge C18 3.5 μm 4.6 \times 150 mm, column oven; 50 °C, monitor; 254 nm, flow rate; 1 mL/min, solvents; (A) 0.1 M TEAA buffer (pH 7.0), (B) MeCN, B conc.; 5–18%/20 min.

The product ratios obtained after a 6-hour treatment using all AP/X combinations with the ^SG -n3-ligand and ^SG -n5-ligand are summarized in Fig. 2H and I, respectively, Fig. 2H shows that the adduct selectivity for the opposing base at the AP site was low. In contrast, Fig. 2I clearly displays a higher ability of the ^SG -n5-ligand for the adduct formation of DNA8. In particular, the pyrimidine bases, dC and dT, produced DNA8 in a higher ratio than the purine bases. The flexible pentyl linker of the ^SG -n5-ligand may allow appropriate movements for the thioguanine to attach the β -eliminated DNA4 at the nick space formed by the DNA1 cleavage, for which an opposing pyrimidine base may form more space than a purine base.

To confirm the adduct formation, we also analyzed the reaction by HPLC using the duplex formed with DNA1(AP) and DNA2(C) (Fig. 3). All the peaks were isolated and their structures were assigned based on the molecular masses determined by MALDI-TOF/MS (Table 4 and Fig. S5). After a 24-hour treatment, DNA5 (MS 5969.87) corresponding to the fragment formed via β -elimination of DNA1 and DNA2 gave the major peaks (Fig. 3A). Although the δ -eliminated fragment DNA7, β -eliminated fragment DNA4 and the adduct DNA8 with the ^SG -n3-ligand were not separated by HPLC, their formations were evidenced by the mass spectrum of Peak3 (Fig. 3A, Table 4 and Fig. S5). In the reaction with the ^SG -n5-ligand, DNA4, 7 or 8 gave separated peaks of the ^SG -n3-ligand and their formations were clear in the mass spectrum (Fig. 3B). In a control experiment using the G-n3-ligand, only DNA4 and 7 were detected in the mass spectrum (Fig. 3C), indicating that the

Table 4
MALDI-TOF/MS of the isolated peaks 1–3.

	Peak	DNA	Calcd. [M-H] ⁻	Found
X = C, ^SG -n3-ligand	1	DNA5	5970.0	5969.9
	2	DNA 2(C)	9027.5	9027.4
	3	DNA4 DNA7 DNA8	3813.2 3713.6 4149.9	3830.2 ^a 3713.9 4150.4
X = C, ^SG -n5-ligand	1	DNA5	5970.0	5970.2
	2	DNA2(C)	9027.5	9024.6
	3	DNA4 DNA7 DNA8	3813.2 3713.6 4177.9	3830.8 ^a 3713.6 4179.1
	X = C, G-n3-ligand	1	DNA5	5970.0
2		DNA2(C)	9027.5	9028.5
3		DNA4 DNA7	3813.2 3713.6	3831.8 ^a 3717.4

^a DNA4 was detected as a hydrate.²⁴

thioguanine is the major contributor of the adduct formation. The results that the guanine base did not form the adduct in this study (Figs. 2B and C) indicate that the 2-amino group of the guanine base did not participate in the adduct formation.^{25,26}

3. Conclusion

We have investigated the reactivity of ⁵G-ligands for the duplex having the AP site and demonstrated that the ⁵G-ligands form the photo-adduct in a selective manner for the opposing dC. It was also found that the ⁵G-ligands promote the β-elimination of the AP sites followed by the adduct formation of the β-eliminated DNA fragment with the ⁵G-ligands without UVA irradiation. The ⁵G-n5-ligand is superior to the ⁵G-n3-ligand from the viewpoints of reaction efficiency as well as the selectivity to the opposing dC and dT. It was speculated that the thioguanine in the nick formed by β-elimination is brought into close proximity with the α, β-unsaturated aldehyde due to the flexible pentyl linker. Accordingly, the ⁵G-ligands displayed an interesting adduct forming ability at the AP site, and are expected to enhance the cytotoxicity of a DNA-acting anticancer drug through a function as the 3'-block for the repair of AP sites and subsequent polymerization.

4. Experimental

4.1. Method

Melting points were determined using a Stuart Scientific MELTING POINT APPARATUS SMP 3. ¹H spectra were recorded at 500 MHz on a Bruker Ascend 500 using CDCl₃ or DMSO as a solvent. ¹³C NMR spectra were recorded at 125 MHz on a Bruker Ascend 500 using CDCl₃ or DMSO as a solvent. Chemical shifts are reported in ppm, in δ units. ESI-MS spectra were recorded on a Bruker micrOTOF II-SKF instrument. IR spectra were recorded on a PerkinElmer Spectrum One FT-IR spectrometer.

4.2. Synthesis of the ligands

4.2.1. *tert*-butyl (3-aminopropyl)(3-((*tert*-butoxycarbonyl)amino)-propyl) carbamate (**2**)

A solution of ethyl trifluoroacetate (8.40 mL, 70.9 mmol) in MeOH (50.0 mL) was dropwise added over a period of 3 h a solution of 3,3'-diaminodipropylamine (10.0 mL, 70.9 mmol) in MeOH (120 mL) at -78 °C. The reaction mixture was stirred for 30 min at -78 °C, then raised to 0 °C. A solution of di-*tert*-butyl dicarbonate (57.0 mL, 248 mmol) in MeOH (40.0 mL) was dropwise added the reaction mixture, and this mixture was stirred for 4 h at rt. MeOH was evaporated and the residue was dissolved in THF (60.0 mL), then aq. LiOH (120 mL) was added to the solution. The reaction mixture was stirred overnight at rt, then neutralized. CHCl₃ (200 mL × 2) was poured into the solution and washed with H₂O (120 mL), brine (200 mL). The organic extracts were dried over anhydrous Na₂SO₄, filtered and evaporated to afford a yellow viscous crude product (33.6 g), which was purified by column chromatography (silica gel, CHCl₃ : MeOH : 28% aq-NH₃ = 180 : 20 : 1 to 90 : 10 : 1) to yield a pale yellow viscous product **2** (13.4 g, 40.6 mmol, 57%). ¹H NMR (500 MHz, CDCl₃) δ ppm: 5.27 (1H, bs), 3.28–3.17 (4H, m), 3.12–3.07 (2H, m), 2.68 (2H, t, *J* = 7 Hz), 1.68–1.61 (4H, m), 1.45 (9H, s), 1.42 (9H, s). ¹³C NMR (125 MHz, CDCl₃) δ ppm: 156.2, 79.8, 79.1, 44.5, 43.8, 39.5, 37.6, 32.7, 31.8, 28.6. HR ESI-MS *m/z*: 332.259 [M + H]⁺ (332.254 calculated for C₁₆H₃₃N₃O₄). IR cm⁻¹: 1676, 1481, 1421, 1366, 1251, 1167.

4.2.2. *tert*-butyl (3-((*tert*-butoxycarbonyl)amino)-propyl)(3-((2-nitrophenyl)sulfonamido)propyl)-carbamate (**3**)

Dry Et₃N (26.0 mL, 186 mmol) and 2-nitrobenzenesulfonyl chloride (9.10 g, 41.0 mmol) were added to a solution of **2** (12.4 g, 37.3 mmol) in anhydrous CH₂Cl₂ (65.3 mL) under an argon atmosphere at 0 °C. The

reaction mixture was stirred for 1 h at 0 °C, then poured CH₂Cl₂ (90.0 mL), washed with 1 M KH₂PO₄ aq. (100 mL), sat. aq. NaHCO₃ (100 mL), and brine (100 mL). The organic extracts were dried over anhydrous Na₂SO₄, filtered and evaporated to afford an orange viscous crude product (18.3 g), which was purified by column chromatography (silica gel, CHCl₃ : EtOAc = 5 : 1 to 3 : 1) to yield a pale yellow foam product **3** (14.5 g, 28.0 mmol, 75%). ¹H NMR (500 MHz, DMSO) δ ppm: 8.05 (1H, bs), 8.01–7.95 (2H, m), 7.88–7.84 (2H, m), 6.72 (1H, bs), 3.08 (2H, t, *J* = 7 Hz), 3.03 (2H, t, *J* = 7 Hz), 2.88–2.84 (4H, m), 1.60 (2H, bs), 1.52–1.49 (2H, m), 1.37 (9H, s), 1.34 (9H, s). ¹³C NMR (125 MHz, DMSO) δ ppm: 155.5, 154.6, 147.8, 134.0, 132.6, 129.4, 124.4, 78.5, 77.5, 44.2, 40.6, 37.6, 28.6, 28.2, 28.0. HR ESI-MS *m/z*: 517.231 [M + H]⁺ (517.233 calculated for C₂₂H₃₆N₄O₈S). IR cm⁻¹: 1681, 1542, 1420, 1366, 1251, 1166.

4.2.3. *tert*-butyl (3-((*N*-(3-bromopropyl)-2-nitro-phenyl)sulfonamido-propyl)(3-((*tert*-butoxy-carbonyl)amino)propyl)carbamate (**4a** (*n* = 3))

A solution of **3** (11.0 g, 21.3 mmol) in dry MeCN (39.0 mL) was added to a suspension of K₂CO₃ (14.7 g, 107 mmol) and 1, 3-dibromopropane (10.9 mL, 107 mmol) under an argon atmosphere at 0 °C. The reaction mixture was stirred at 50 °C overnight, then filtered. The filtrate was evaporated and dissolved in CHCl₃ (100 mL), washed with H₂O (50.0 mL) and brine (50.0 mL). The organic extracts were dried over anhydrous Na₂SO₄, filtered and evaporated to afford a clear pale yellow oil crude product (25.0 g), which was purified by column chromatography (silica gel, CHCl₃ : EtOAc = 10 : 1 to 6 : 1) to yield a pale yellow viscous product **4a** (*n* = 3) (9.10 g, 14.3 mmol, 67%). ¹H NMR (500 MHz, CD₃Cl₃) δ ppm: 8.03 (1H, d, *J* = 7 Hz), 7.73–7.67 (2H, m), 7.63 (1H, d, *J* = 7 Hz), 3.44 (2H, t, *J* = 7 Hz), 3.38 (2H, t, *J* = 6 Hz), 3.31 (2H, t, *J* = 8 Hz), 3.21 (2H, t, *J* = 6 Hz), 3.15 (2H, bs), 3.07 (2H, bs), 2.11 (2H, quint., *J* = 6 Hz), 1.80 (2H, quint., *J* = 7 Hz), 1.63 (2H, bs), 1.45 (9H, s), 1.43 (9H, s). ¹³C NMR (125 MHz, CDCl₃) δ ppm: 156.2, 148.2, 133.9, 133.2, 131.9, 131.2, 124.4, 79.1, 45.9, 44.5, 37.5, 31.4, 30.0, 28.6, 27.4. HR ESI-MS *m/z*: 637.190, 639.188 [M + H]⁺ (637.190, 639.188 calculated for C₂₅H₄₁BrN₄O₈S). IR cm⁻¹: 2975, 1686, 1545, 1418, 1366, 1160.

4.2.4. *tert*-butyl (3-((*N*-(5-bromopentyl)-2-nitro-phenyl)sulfonamido-propyl)(3-((*tert*-butoxy-carbonyl)amino)propyl)carbamate (**4b** (*n* = 5))

K₂CO₃ (2.17 g, 15.7 mmol) and a solution of **3** (2.70 g, 5.23 mmol) in dry DMF (6.00 mL) were added to 1, 5-dibromo-pentane (3.60 mL, 26.1 mmol) under an argon atmosphere at 0 °C. The reaction mixture was stirred at rt overnight, then poured ether (40.0 mL × 2), washed with H₂O (60.0 mL) and brine (50.0 mL). The organic extracts were dried over anhydrous Na₂SO₄, filtered and evaporated to afford a clear yellow oil crude product (8.19 g), which was purified by column chromatography (silica gel, CHCl₃ : EtOAc = 10 : 1) to yield a yellow viscous product **4b** (*n* = 5) (3.20 g, 4.85 mmol, 93%). ¹H NMR (500 MHz, CD₃Cl₃) δ ppm: 8.00 (1H, bs), 7.71–7.66 (2H, m), 7.62 (1H, d, *J* = 8 Hz), 3.35 (2H, t, *J* = 7 Hz), 3.31–3.27 (4H, m), 3.20 (2H, t, *J* = 6 Hz), 3.13 (2H, bs), 3.07 (2H, bs), 1.85–1.77 (4H, m), 1.62–1.52 (4H, m), 1.45 (9H, s), 1.43 (9H, s), 1.41–1.39 (2H, m). ¹³C NMR (125 MHz, CDCl₃) δ ppm: 156.1, 148.2, 133.7, 133.6, 131.8, 130.9, 124.3, 80.1, 79.2, 47.2, 45.2, 44.5, 44.1, 37.6, 33.5, 32.2, 28.6, 27.4, 25.2. HR ESI-MS *m/z*: 687.207, 689.205 [M + H]⁺ (687.203, 689.202 calculated for C₂₇H₄₅BrN₄O₈S). IR cm⁻¹: 2932, 1683, 1545, 1366, 1160.

4.2.5. *tert*-butyl (3-((*N*-(3-(2-amino-6-chloro-9H-purin-9-yl)propyl)-2-nitrophenyl)sulfonamide-propyl)(3-((*tert*-butoxycarbonyl)amino)propyl)-carbamate (**5a** (*n* = 3))

2-Amino-6-chloropurine (2.20 g, 12.8 mmol) and K₂CO₃ (3.54 g, 25.6 mmol) were added to a solution of **4a** (*n* = 3) (9.00 g, 14.1 mmol) in anhydrous DMF (15.0 mL) under an argon atmosphere at 0 °C. The reaction mixture was stirred at rt overnight, then poured H₂O (100 mL), extracted with CHCl₃ (100 mL) and washed with brine (100 mL). The

organic extracts were dried over anhydrous Na_2SO_4 , filtered and evaporated to afford a brown viscous crude product (15.7 g), which was purified by column chromatography (silica gel, CHCl_3 : MeOH = 60 : 1 to 20 : 1) to yield a pale yellow foam product **5a** ($n = 3$) (7.60 g, 10.5 mmol, 82%). ^1H NMR (500 MHz, DMSO) δ ppm: 8.11 (1H, s), 7.96 (1H, d, $J = 8$ Hz), 7.91 (1H, d, $J = 8$ Hz), 7.87 (1H, t, $J = 8$ Hz), 7.79 (2H, t, $J = 8$ Hz), 6.88 (2H, s), 6.72 (1H, bs), 4.04 (2H, t, $J = 7$ Hz), 3.33 (2H, t, $J = 8$ Hz), 3.03 (2H, t, $J = 7$ Hz), 2.85 (2H, q, $J = 7$ Hz), 2.05 (2H, quint., $J = 7$ Hz), 1.50–1.49 (2H, m), 1.36 (9H, s), 1.33 (9H, bs). ^{13}C NMR (125 MHz, DMSO) δ ppm: 160.2, 156.0, 154.5, 149.8, 148.0, 143.5, 135.1, 132.9, 131.9, 130.1, 124.9, 123.9, 79.0, 77.9, 45.7, 45.3, 44.5, 41.0, 38.1, 28.7, 28.4, 28.2. HR ESI-MS m/z : 726.283 $[\text{M} + \text{H}]^+$ (726.280 calculated for $\text{C}_{30}\text{H}_{44}\text{ClN}_9\text{O}_8\text{S}$). IR cm^{-1} : 1678, 1613, 1545, 1367, 1161.

4.2.6. *tert*-butyl (3-((*N*-(5-(2-amino-6-chloro-9H-purin-9-yl)pentyl)-2-nitrophenyl)sulfonamido)propyl)(3-((*tert*-butoxycarbonyl)amino)propyl)carbamate (**5b** ($n = 5$))

Compound **5b** ($n = 5$) was prepared using compound **4b** ($n = 5$) (3.20 g, 4.81 mmol) and the other reagents described above. An orange viscous crude product (5.66 g), which was purified by column chromatography (silica gel, CHCl_3 : MeOH = 60 : 1 to 20 : 1) to yield a pale yellow viscous product **5b** ($n = 5$) (2.50 g, 3.25 mmol, 74%). ^1H NMR (500 MHz, DMSO) δ ppm: 8.10 (1H, s), 7.98–7.94 (2H, m), 7.87 (1H, dt, $J = 2, 8$ Hz), 7.82 (2H, t, $J = 2, 8$ Hz), 6.87 (2H, s), 6.72 (1H, bs), 4.00 (2H, t, $J = 7$ Hz), 3.24 (2H, t, $J = 8$ Hz), 3.19 (2H, t, $J = 8$ Hz), 3.05–3.02 (4H, m), 2.86 (2H, q, $J = 6$ Hz), 1.75 (2H, quint., $J = 7$ Hz), 1.64–1.62 (2H, m), 1.52–1.50 (4H, m), 1.36 (9H, s), 1.33 (9H, s), 1.23–1.14 (2H, m). ^{13}C NMR (125 MHz, DMSO) δ ppm: 159.7, 155.5, 154.5, 154.0, 149.3, 147.5, 143.1, 134.4, 132.4, 131.8, 129.6, 124.3, 123.3, 78.5, 77.4, 47.1, 45.0, 44.1, 42.8, 37.6, 28.5, 28.2, 28.0, 27.4, 23.0. HR ESI-MS m/z : 754.312 $[\text{M} + \text{H}]^+$ (754.311 calculated for $\text{C}_{32}\text{H}_{48}\text{ClN}_9\text{O}_8\text{S}$). IR cm^{-1} : 1673, 1615, 1545, 1367, 1161.

4.2.7. *tert*-butyl (3-((*N*-(3-(2-amino-6-thioxo-1,6-dihydro-9H-purin-9-yl)propyl)-2-nitrophenyl)sulfonamido)propyl)(3-((*tert*-butoxycarbonyl)amino)propyl)carbamate (**6a** ($n = 3$))

Thiourea (786 mg, 10.3 mmol) was added to a solution of **5a** ($n = 3$) (2.50 g, 3.44 mmol) in ethanol (46.0 mL) at rt. The reaction mixture was refluxed for 2 h, then the solvent was evaporated. The residue was dissolved in EtOAc (100 mL \times 3), and washed with H_2O (150 mL). The organic extracts were dried over anhydrous Na_2SO_4 , filtered and evaporated to afford a yellow foam crude product (2.30 g), which was purified by column chromatography (silica gel, CHCl_3 : MeOH = 40 : 1 to 10 : 1) to yield a yellow solid product **6a** ($n = 3$) (1.80 g, 2.50 mmol, 73%). ^1H NMR (500 MHz, DMSO) δ ppm: 11.86 (1H, s), 7.96 (1H, dd, $J = 1, 8$ Hz), 7.89–7.85 (2H, m), 7.86 (1H, s), 7.79 (1H, dt, $J = 1, 8$ Hz), 6.75 (3H, bs), 3.95 (2H, t, $J = 7$ Hz), 3.31 (2H, t, $J = 8$ Hz), 3.23 (2H, t, $J = 8$ Hz), 3.05–3.02 (4H, m), 2.86 (2H, q, $J = 6$ Hz), 1.99 (2H, quint., $J = 7$ Hz), 1.63 (2H, quint., $J = 7$ Hz), 1.50–1.49 (2H, m), 1.36 (9H, s), 1.35 (9H, bs). ^{13}C NMR (125 MHz, DMSO) δ ppm: 174.9, 155.5, 154.6, 152.9, 147.8, 147.5, 140.3, 134.6, 132.4, 131.5, 129.6, 128.3, 124.4, 78.5, 77.5, 45.2, 44.8, 44.0, 40.3, 37.6, 28.8, 28.3, 28.0, 27.1. HR ESI-MS m/z : 724.288 $[\text{M} + \text{H}]^+$ (724.291 calculated for $\text{C}_{30}\text{H}_{45}\text{N}_9\text{O}_8\text{S}_2$). IR cm^{-1} : 1676, 1632, 1579, 1542, 1367, 1161.

4.2.8. *tert*-butyl (3-((*N*-(5-(2-amino-6-thioxo-1,6-dihydro-9H-purin-9-yl)pentyl)-2-nitrophenyl)sulfonamido)propyl)(3-((*tert*-butoxycarbonyl)amino)propyl)carbamate (**6b** ($n = 5$))

Compound **6b** ($n = 5$) was prepared using compound **5b** ($n = 5$) (2.50 g, 3.25 mmol) and the other reagents describe above. A yellow foam crude product (2.07 g), which was purified by column chromatography (silica gel, CHCl_3 : MeOH = 40 : 1 to 20 : 1) to yield a yellow foam product **6b** ($n = 5$) (1.94 g, 2.58 mmol, 80%). ^1H NMR (500 MHz, DMSO) δ ppm: 11.85 (1H, bs), 7.98–7.94 (2H, m), 7.88–7.80 (2H, m),

7.85 (1H, s), 6.75 (2H, bs), 6.73 (1H, bs), 3.91 (2H, t, $J = 7$ Hz), 3.25–3.16 (4H, m), 3.06–3.03 (4H, m), 2.86 (2H, q, $J = 6$ Hz), 1.70 (2H, quint., $J = 7$ Hz), 1.63 (2H, quint., $J = 7$ Hz), 1.53–1.47 (4H, m), 1.34 (9H, s), 1.33 (9H, s), 1.16 (2H, quint., $J = 8$ Hz). ^{13}C NMR (125 MHz, DMSO) δ ppm: 174.8, 155.5, 154.6, 152.9, 147.8, 147.5, 140.5, 134.4, 132.4, 131.8, 129.6, 128.3, 124.3, 78.5, 77.5, 47.1, 45.0, 44.1, 42.6, 37.6, 28.7, 28.2, 28.0, 27.4, 23.0. HR ESI-MS m/z : 752.320 $[\text{M} + \text{H}]^+$ (752.322 calculated for $\text{C}_{32}\text{H}_{49}\text{N}_9\text{O}_8\text{S}_2$). IR cm^{-1} : 1682, 1635, 1580, 1543, 1367, 1161.

4.2.9. 2-amino-9-(3-((3-((3-aminopropyl)amino)propyl)amino)propyl)-1,9-dihydro-6H-purine-6-thione (**7a** ($n = 3$)); $^5\text{G-n3}$ -ligand

K_2CO_3 (1.03 g, 7.47 mmol) and thiophenol (281 μL , 2.74 mmol) were added to a solution of **6a** ($n = 3$) (1.80 g, 2.49 mmol) in anhydrous DMF (4.20 mL) under an argon atmosphere at 0 °C. The reaction mixture was stirred for 4 h at rt, then evaporated to afford a dark orange viscous crude product (3.70 g), which was purified by column chromatography (silica gel, CHCl_3 : MeOH : 28% aq- $\text{NH}_3 = 90 : 10 : 1$ to 40 : 8 : 1) to yield a yellow viscous product (1.26 g, 2.35 mmol, 94%). ^1H NMR (500 MHz, DMSO) δ ppm: 7.85 (1H, s), 6.75 (3H, bs), 3.99 (2H, t, $J = 7.0$ Hz), 3.13–3.07 (4H, m), 2.88 (2H, q, $J = 6$ Hz), 1.83 (2H, quint., $J = 7$ Hz), 1.57–1.54 (4H, m), 1.37 (9H, s), 1.36 (9H, s). ^{13}C NMR (125 MHz, DMSO) δ ppm: 174.9, 155.6, 154.7, 152.9, 147.8, 140.6, 128.3, 78.3, 77.5, 46.7, 46.0, 44.4, 44.2, 40.9, 37.6, 29.4, 28.8, 28.3, 28.1. HR ESI-MS m/z : 539.309 $[\text{M} + \text{H}]^+$ (539.312 calculated for $\text{C}_{24}\text{H}_{42}\text{N}_8\text{O}_4\text{S}$). IR cm^{-1} : 1678, 1578, 1421, 1391, 1366, 1251, 1171.

This Nosyl deprotected **6a** ($n = 3$) (1.25 g, 2.32 mmol) was dissolved in 0.5 M HCl/MeOH (46.0 mL, 23.2 mmol) and the reaction mixture was stirred for 6 days at rt. The precipitates were collected on the filter, and washed with cold HCl/MeOH to afford a crude product, which was purified by precipitation from water/EtOH (2.20 mL/40.0 mL) at -78 °C. The purified **7a** ($n = 3$) was collected by centrifuging (1,500 rpm, 10 min), and the supernatant removed using a pipette. The precipitate was dried under vacuum to give **7a** ($n = 3$) as a pale yellow solid (1.00 g, quant.). m.p. 279–283 °C. ^1H NMR (500 MHz, DMSO) δ ppm: 12.70 (1H, s), 9.44–9.40 (4H, m), 9.00 (1H, s), 8.22 (3H, bs), 7.47 (2H, bs), 4.23 (2H, t, $J = 6$ Hz), 3.01–2.97 (6H, m), 2.92–2.91 (4H, m), 2.22 (2H, quint., $J = 7$ Hz), 2.09 (2H, quint., $J = 7$ Hz), 2.01 (2H, quint., $J = 7$ Hz). ^{13}C NMR (125 MHz, DMSO) δ ppm: 173.4, 154.4, 146.5, 140.2, 122.2, 44.0, 43.9, 43.8, 41.5, 36.1, 25.2, 23.6, 22.2. HR ESI-MS m/z : 339.212 $[\text{M} + \text{H}]^+$ (339.207 calculated for $\text{C}_{14}\text{H}_{26}\text{N}_8\text{S}$). IR cm^{-1} : 2972, 2767, 1645, 1618, 1594.

4.2.10. 2-amino-9-(5-((3-((3-aminopropyl)amino)propyl)amino)pentyl)-1,9-dihydro-6H-purine-6-thione (**7b** ($n = 5$)); $^5\text{G-n5}$ -ligand

K_2CO_3 (1.04 g, 7.55 mmol) and thiophenol (284 μL , 2.77 mmol) were added to a solution of **6b** ($n = 5$) (1.89 g, 2.52 mmol) in dry DMF (5.00 mL) under an argon atmosphere at 0 °C. The reaction mixture was stirred for 4 h at rt, then poured H_2O (50.0 mL), extracted with EtOAc (150 mL \times 2) and washed with brine (80.0 mL). The organic extracts were dried over anhydrous Na_2SO_4 , filtered and evaporated to afford an orange viscous crude product (3.13 g), which was purified by column chromatography (silica gel, CHCl_3 : MeOH : 28% aq- $\text{NH}_3 = 90 : 10 : 1$ to 40 : 8 : 1) to yield a white foam product (1.29 g, 2.28 mmol, 91%). ^1H NMR (500 MHz, DMSO) δ ppm: 7.88 (1H, s), 6.77 (2H, bs), 6.75 (1H, bs), 3.93 (2H, t, $J = 7$ Hz), 3.14–3.07 (4H, m), 2.88 (2H, q, $J = 6$ Hz), 2.48–2.44 (4H, m), 1.72 (2H, quint., $J = 7$ Hz), 1.60–1.56 (4H, m), 1.41 (2H, quint., $J = 7$ Hz),

1.37 (9H, s), 1.36 (9H, s), 1.23 (2H, quint., $J = 8$ Hz). ^{13}C NMR (125 MHz, DMSO) δ ppm: 174.9, 155.6, 154.7, 152.9, 147.8, 140.6, 128.3, 78.3, 77.5, 48.9, 46.5, 44.3, 42.7, 37.6, 29.1, 28.5, 28.2, 28.1, 27.7, 23.8. HR ESI-MS m/z : 567.348 $[\text{M} + \text{H}]^+$ (567.344 calculated for $\text{C}_{26}\text{H}_{46}\text{N}_8\text{O}_4\text{S}$). IR cm^{-1} : 1682, 1576, 1391, 1366, 1251, 1167.

This Nosyl deprotected **6b** ($n = 5$) (1.28 g, 2.26 mmol) was dissolved in 0.5 M HCl/MeOH (45.0 mL, 22.6 mmol) and the reaction mixture was stirred for 6 days at rt. The precipitates were collected on

the filter, and washed with cold HCl/MeOH to afford a crude product, which was purified by precipitation from water/EtOH (2.30 mL/45.0 mL) at -78°C . The purified **7b** ($n = 5$) was collected by centrifuging (1,500 rpm, 10 min), and the supernatant removed using a pipette. The precipitate was dried under vacuum to give **7b** ($n = 5$) as a pale yellow solid (899 mg, 1.75 mmol, 78%). m.p. 265–268 $^{\circ}\text{C}$. ^1H NMR (500 MHz, DMSO) δ ppm: 12.48 (1H, s), 9.31 (2H, bs), 9.17 (2H, bs), 8.69 (1H, s), 8.15 (3H, bs), 7.29 (2H, bs), 4.04 (2H, t, $J = 7$ Hz), 3.05–2.95 (6H, m), 2.93 (2H, q, $J = 6$ Hz), 2.90–2.81 (2H, m), 2.07 (2H, quint., $J = 7$ Hz), 2.00 (2H, quint., $J = 7$ Hz), 1.80 (2H, quint., $J = 7$ Hz), 1.69 (2H, quint., $J = 8$ Hz), 1.30 (2H, quint., $J = 8$ Hz). ^{13}C NMR (125 MHz, DMSO) δ ppm: 173.4, 154.1, 146.8, 140.4, 123.5, 46.5, 44.1, 44.0, 43.9, 43.5, 36.2, 28.2, 24.8, 23.7, 22.9, 22.2. HR ESI-MS m/z : 367.238 $[\text{M} + \text{H}]^+$ (367.239 calculated for $\text{C}_{16}\text{H}_{30}\text{N}_8\text{S}$). IR cm^{-1} : 2975, 1645, 1588, 1453, 1198, 1172.

4.3. Synthesis of ODNs containing the AP site analogue.

Complementary oligodeoxynucleotides (ODNs) (5'-d(CGC ATY₂ Z X₂TA CGC)-3') were purchase from Japan Bio Services Co., LTD. (Saitama, JAPAN) or Life Technologies Japan Ltd (Tokyo, JAPAN). ODNs containing the AP site analogue were synthesized using solid phase phosphoramidite chemistry on a NIHON TECHNO SERVICE H-Series synthesizer. The cleaved oligonucleotides were purified by HPLC on a COSMOSIL 5C18-MS-II column using a linear gradient between the 0.1 M TEAA buffer and CH_3CN . The MALDI-TOF/MS was measured on a BRUKER DALTONICS microflex-KS spectrometer with matrix containing 3-hydroxy-2-picolinic acid and diammonium hydrogen citrate solution. These data were summarized in Table 2. Oligonucleotide concentrations were determined spectrophotometrically by measuring the absorbance at 260 nm.

4.4. Evaluation of the stability of duplex ODNs containing the AP site analogue with $^{\text{S}}\text{G}$ -ligands by thermal denaturation studies

All duplexes melting curves were measured on a UV BECKMAN COULTER DU800 in the absence and presence of 10 μM ligand, at a concentration of 2 μM duplex in the buffer containing 10 mM HEPES-NaOH (pH 7.0), 100 mM NaCl at a heat rate of 1 $^{\circ}\text{C}/\text{min}$ (from 20 $^{\circ}\text{C}$ to 80 $^{\circ}\text{C}$) and a scan rate of 1 $^{\circ}\text{C}/\text{min}$. As a pretreatment, all samples were heated for 5 min at 80 $^{\circ}\text{C}$ and then gradually cooled down. Obtained melting curves were analyzed by non-linear fitting and each melting temperature was determined. $\Delta T_m = T_m(+)-T_m(-)$, which were summarized in Table 1. Table 3 summarized the ΔT_m values obtained using the full matched duplexes. The average mean and the standard deviation, $\Delta T_m (\pm \text{SD})$, were calculated based on three times independent experiments.

4.5. Evaluation of the photoreaction of duplex ODNs containing the AP site analogue with $^{\text{S}}\text{G}$ -ligands and G-n3-ligand by UVA irradiation

The photo-crosslinking reaction was performed by UVA irradiation (4 W, 365 nm, Funakoshi UVGL-25) at the concentration of 10 μM duplex and 100 μM $^{\text{S}}\text{G}$ -ligand in the buffer containing 10 mM HEPES-NaOH (pH 7.0), 5 mM DTT and 100 mM NaCl. The reaction mixtures were irradiated at rt for 24 h, then these samples were analyzed by HPLC using the following conditions. Column: Waters X Bridge C18 3.5 μm , 4.6 \times 150 mm; column oven: 50 $^{\circ}\text{C}$; UV monitor at 254 nm; flow rate: 1 mL/min; solvents: A) 0.1 M TEAA buffer (pH 7.0), B) MeCN, B 4% to 14%/15 min. (3% to 16%/15 min for Fig. 1F). The HPLC chart were summarized in Fig. 1. The time course of photoreaction between duplex 4 and $^{\text{S}}\text{G}$ -n3-ligand was shown in Fig. S1. The peak marked with (*) was isolated by same HPLC conditions as above and measured MALDI-TOF MS using matrix containing 3-hydroxy-2-picolinic acid and diammonium hydrogen citrate solution.

4.6. Preparation of duplex ODNs containing the AP site

ODNs were purchase from Life Technologies Japan Ltd. (Tokyo, JAPAN). The single-stranded ODN containing the uracil residue at position 11 of the 30 mer ODN (DNA1(U); 5' FAM-d(GTT GGA GCT GUT GGC GTA GGC AAG AGT GCC)-3') was labeled at the 5'-end with 6-carboxyfluorescein (6-FAM). The DNA1(U) was annealed at 70 $^{\circ}\text{C}$ for 5 min with DNA2(X) (5'-d(GGC ACT CTT GCC TAC GCC AXC AGC TCC AAC)-3', X = A, G, C, T). The annealed duplex ODN was treated with 0.2 unit/ μl uracil-DNA glycosylase (NEW ENGLAND BioLabs) in 50 mM HEPES-NaOH buffer (pH 7.4), 1 mM EDTA, and 1 mM DTT at 37 $^{\circ}\text{C}$ for 15 min to create the DNA1(AP)/DNA2(X) duplex having an AP site, which was purified by the Micro Bio-Spin® P-30 column.

4.7. Evaluation of cleavage and adduct forming ability of ODNs containing the AP site with $^{\text{S}}\text{G}$ -ligands by gel-electrophoresis

The DNA1(U)/DNA2(X) duplex (100 nM) was prepared as described above. The sample was annealed again in 10 mM HEPES-NaOH buffer containing 100 mM NaCl at 70 $^{\circ}\text{C}$ and pH 7.0 for 5 min, then incubated with the $^{\text{S}}\text{G}$ -ligands (10 μM) at 37 $^{\circ}\text{C}$ for 5, 10, 15, 30, 60, 120, 180, 240, or 300 min. The reaction mixture was quenched by the addition of the loading buffer (5 M urea, 10 mM EDTA, TBE buffer, and 0.025 w/v % xylene cyanol in final concentration) on ice. The cleaved fragments of DNA1(AP) were resolved by 12% denaturing polyacrylamide gel electrophoresis containing 8 M urea at 25 mA for 40 min. The gel was visualized by FAM fluorescence using LAS-4000. The results are summarized in Fig. 2 and Figure S2. The time course of ratio of the DNA fragments were calculated using ImageJ.

4.8. Evaluation of cleavage and adduct forming ability of ODNs containing the AP site with $^{\text{S}}\text{G}$ -ligands and G-n3-ligand by HPLC

The DNA1(U)/DNA2(C) duplex (22 μM) was prepared as described above in 10 mM HEPES-NaOH buffer containing 100 mM NaCl at 70 $^{\circ}\text{C}$ and pH 7.0 for 5 min, then incubated with the $^{\text{S}}\text{G}$ -ligand (220 μM) at 37 $^{\circ}\text{C}$ for 1, 3, 6, or 24 h. The reaction mixture was stored at -30°C . These samples were analyzed by HPLC using the following conditions. Column: Waters X Bridge C18 3.5 μm , 4.6 \times 150 mm; column oven: 50 $^{\circ}\text{C}$; UV monitor at 254 nm; flow rate: 1 mL/min; solvents: A) 0.1 M TEAA buffer (pH 7.0), B) MeCN, B 5% to 18%/20 min. The HPLC charts are summarized in Fig. 3. Peaks 1–3 were isolated and their structure were determined by MALDI-TOF/MS measurements, which are summarized in Fig. S5. The DNA4 was detected as hydrated product ($+\text{H}_2\text{O}$).²⁴

Declaration of Competing Interest

The author declare that there is no conflict of interest.

Acknowledgments

This study was supported by a Grant-in-Aid for Scientific Research (B) (Grant Number 15H04633 for S. S.) and a Grant-in-Aid for Young Scientists (B) (Grant Number 26860079 for Y. A.) from the Japan Society for Promotion of Science (JSPS).

Appendix A. Supplementary material

Supplementary data to this article can be found online at <https://doi.org/10.1016/j.bmc.2019.115160>.

References

- Barnett RN, Cleveland CL, Landman U. *ACC Chem. Res.* 2010;43:280–287.
- Drabløs F, Feyzi E, Aas PA, et al. *DNA Repair.* 2004;3:1389–1407.

3. Lindahl T, Karran P, Wood RD. *Curr. Opin. Genet. Dev.* 1997;7:158–169.
4. Friedman JI, Stivers JT. *Biochemistry.* 2010;49:4957–4967.
5. Baldwin MR, O'Brien PJ. *Biochemistry.* 2010;49:7879–7891.
6. Lhomme J, Constant J-F, Demeunynck M. *Biopolymers.* 1999;52:65–83.
7. Fishel ML, Kelly MR. *Mol. Aspects Med.* 2007;28:375–395.
8. Fkyerat A, Demeunynck M, Constant J-F, Michon P, Lhomme J. *J. Am. Chem. Soc.* 1993;115:9952–9959.
9. Malina J, Scott P, Brabec V. *Nucleic Acids Res.* 2015;43:5297–5306.
10. Kotera N, Poyer F, Granzhan A, Teulade-Fichou M-P. *Chem. Commun.* 2015;51:15948–15951.
11. Caron C, Duong XNT, Guillot R, Bomberd S, Granzhan A. *Chem. Eur. J.* 2019;25:1949–1962.
12. Minko IG, Jacobs AC, de Leon AR, et al. *Sci Rep.* 2016;6:28894.
13. Abe Y, Nakagawa O, Yamaguchi R, Sasaki S. *Bioorg. Med. Chem.* 2012;20:3470–3479.
14. Abe SY, Sasaki S. *Bioorg. Med. Chem.* 2016;24:910–914.
15. Favre A, Saintomé C, Fourrey J-L, Clivio P, Laugãa PJ. *Photochem. Photobiol. B Biol.* 1998;42:109–124.
16. Brem R, Karran P. *Photochem. Photobiol.* 2012;88:5–13.
17. Špačková N, Cubero L, Šponer J, Orozco M. *J. Am. Chem. Soc.* 2004;126:14642–14650.
18. Somerville L, Krynetski EY, Krynetskaia NF, et al. *J. Biol. Chem.* 2003;278:1005–1011.
19. SantaLucia Jr J. *Proc. Natl. Acad. Sci. USA.* 1998;95:1460–1465.
20. Nishioka T, Oshiro I, Onizuka K, Taniguchi Y, Sasaki S. *Chem. Pharm. Bull.* 2016;64:1315–1320.
21. Bailly V, Derydt M, Verly WG. *Biochem. J.* 1989;261:707–713.
22. Bailly V, Verly WG. *Nucleic Acids Res.* 1988;16:9489–9496.
23. Mahugh PJ, Knowland J. *Nucleic Acids Res.* 1995;23:1664–1670.
24. Sugiyama H, Fujiwara T, Ura A, et al. *Chem. Res. Toxicol.* 1994;7:673–683.
25. Dutta S, Chowdhury G, Gates KS. *J. Am. Chem. Soc.* 2007;129:1852–1853.
26. Johnson KM, Price NE, Wang J, et al. *J. Am. Chem. Soc.* 2013;135:1015–1025.